

First-principles optical spectra of low dimensional systems

Letizia Chiodo^{*,1}, Mauro Bruno¹, Maurizia Palummo¹, and Patrizia Monachesi^{1,2}

¹ European Theoretical Spectroscopy Facility (ETSF) and CNR-INFM, Dipartimento di Fisica, Università di Roma ‘Tor Vergata’, 00133 Roma, Italy

² Dipartimento di Fisica, Università dell’Aquila, 67100 L’Aquila, Italy

Received 15 July 2005, revised 11 October 2005, accepted 12 October 2005

Published online 29 November 2005

PACS 33.20.Lg, 71.15.–m, 78.20.Bh, 78.20.Ci, 78.67.Lt

Low dimensional systems, such as organic molecules, nanotubes, nanowires, have attracted great interest in the last few years, due to their possible application in nanodevices. It is therefore important to describe accurately the electronic excitations, with highly reliable and efficient *ab-initio* approaches. A standard technique for studying the ground-state properties is the Density Functional Theory; however when electronic excited states are involved, the many-body Green’s functions theory is used for obtaining quasi-particle excitation energies and optical spectra. In this paper we will present the current status of this theoretical and computational approach, showing results for a bulk semiconductor and for two different kinds of low dimensional systems.

© 2005 WILEY-VCH Verlag GmbH & Co. KGaA, Weinheim

1 Introduction

Semiconductor device fabrication shows a remarkable trend towards miniaturization, driven by many scientific and technological innovations. The size of device components is now reaching the nanometric scale, i.e. the actual fabrication technological limit. This limitation could be overcome by substituting traditional inorganic semiconductor components with single nanostructures, such as nanowires, nanotubes, or organic molecules. It is therefore important to study these systems in order to understand their properties for possible electronic and optoelectronic applications. In this context, theoretical calculations can help in the interpretation of experimental results, and, more importantly, may be useful in predicting structural, electronic, optical, and transport properties to help to realize more efficient devices.

Density Functional Theory (DFT) [1] is a many-body approach successfully used to calculate the ground-state electronic properties of many-electron systems. However, when physical phenomena involving excited states are studied, it is necessary to include many-body effects not contained in DFT, through Green’s function theory. The use of many-body perturbation theory [2], with DFT calculations as zero order approximation, is nowadays the state-of-the-art to obtain quasi-particle excitation energies and dielectric response in an increasing number of systems, from bulk materials to surfaces and nanostructures. A general discussion of this theoretical framework will be presented in the next section, referring the reader to the books and the reviews available in the literature for a complete description (see, for instance, [3–5]), while some examples of applications to systems of different dimensionality will be given in the last section.

* Corresponding author: e-mail: letizia.chiodo@roma2.infn.it, Phone: +39 06 725 94 741, Fax: +39 06 202 35 07

2 Theoretical framework

The Density Functional Theory, introduced by Hohenberg and Kohn (HK) in 1964 [1], is based on the idea that the ground state energy of a system of N interacting electrons in an external potential $V_{\text{ext}}(\mathbf{r})$ can be written as a functional of the ground state electronic density. In the Kohn and Sham [6] formulation it consists in a self-consistent solution of one-particle effective equations (Kohn–Sham equations):

$$\left[-\frac{1}{2}\nabla^2 + V_{\text{eff}}^{\text{KS}}(\mathbf{r})\right] \cdot \phi_i(\mathbf{r}) = \varepsilon_i \phi_i(\mathbf{r}), \quad (1)$$

where $\rho(\mathbf{r}) = \sum_i^N |\phi_i(\mathbf{r})|^2$ is the electronic charge density and $V_{\text{eff}}^{\text{KS}}(\mathbf{r}) = V_{\text{ext}}(\mathbf{r}) + V_{\text{H}}(\mathbf{r}) + V_{\text{xc}}(\mathbf{r})$. V_{H} is the Hartree potential and V_{xc} is the exchange–correlation potential defined as $V_{\text{xc}} = \delta E_{\text{xc}} / \delta \rho(\mathbf{r})$ which contains all the many-body effects and it is usually calculated in local [7] or semilocal [8] approximations. Being a ‘ground-state’ theory, it can be expected that DFT electronic band structures do not compare very well with experiment. Indeed the calculated electronic band gaps of semiconductors and insulators severely underestimate the experimental ones, and the same happens in molecules for the HOMO-LUMO separation. This is due to the fact that occupied states are experimentally accessible by extracting an electron from the system (direct photoemission) and unoccupied states are accessible by adding one electron (inverse photoemission): in both cases, the system is not in its ground state, but in an excited one. Moreover, even if it were possible to find an exact exchange–correlation potential, there is no rigorous justification to interpret the KS eigenvalues ε_i as the electron addition or removal energies. We will summarize, therefore, in the following, the rigorous method, based on the Green-functions approach, that enables the calculation of electronic band structure. Further information and more details about the Green function approach can be found elsewhere [9–11].

When a bare particle, like an electron or hole, enters an interacting system, it perturbs the particles in its vicinity and it is dressed by a polarization cloud of the surrounding particles, becoming a so-called *quasi-particle*. Using this concept, it is possible to describe the system through a set of *quasi-particle* equations by introducing a non local, time-dependent, non hermitian operator called the *self-energy* Σ , which takes into account the interaction of the particle with the system.

$$\left(-\frac{1}{2}\nabla^2 + V_{\text{ext}} + V_{\text{H}}\right) \Psi_i(\mathbf{r}, \omega) + \int \Sigma(\mathbf{r}, \mathbf{r}', \omega) \Psi_i(\mathbf{r}', \omega) d\mathbf{r}' = E_i(\omega) \Psi_i(\mathbf{r}). \quad (2)$$

Since the operator Σ is not hermitian, the energies $E_i(\omega)$ are in general complex, and the imaginary part of Σ is related to the life time of the excited particle [12]. The most used approximation to calculate the self-energy is nowadays the so-called GW method. It can be derived as the first-step iterative solution of the so-called *Hedin* integral equations (see Ref. [2, 13, 14]) which link the *Green function* G , the *self-energy* Σ , the screened coulomb potential W , the polarization P and the vertex Γ . Actually Eq. (2) is not usually solved directly, thanks to the fact that the Kohn–Sham wavefunctions are often very similar to the GW ones [13]. It is sufficient to calculate the QP corrections in first-order perturbation theory [13, 14]. Moreover the energy dependence of the self-energy is accounted for expanding Σ in Taylor series and the QP corrections are then given by:

$$\Delta \varepsilon_{nk} = \frac{1}{1 + \beta_{nk}} \langle \phi_{nk}^{\text{LDA}} | \Sigma(\varepsilon_{nk}^{\text{LDA}}) - V_{\text{xc}}^{\text{LDA}} | \phi_{nk}^{\text{LDA}} \rangle, \quad (3)$$

where β_{nk} is the linear coefficient in the energy expansion of Σ around the DFT-LDA eigenvalues ε_{nk} .

On the other hand, the physical quantity to be determined in order to obtain the optical spectra is the macroscopic dielectric function $\varepsilon_{\text{M}}(\omega)$, which can be calculated at different levels of accuracy within this theoretical *ab-initio* approach. A relevant component in the interpretation of the optical measurements of reduced dimension systems is the local-field effects (LFE). These effects are important for inhomogeneous systems, where even long wavelength external perturbations produce microscopic fluctuations of the

electric field, which must be taken into account. In low dimensional systems such as surfaces (2D), wires (1D) and isolated molecules (0D) the inhomogeneity of the charge density increases with respect to the solid bulk, and the local-field effects should become more important.

It is known [15] that for inhomogenous materials $\varepsilon_M(\omega)$ is not simply the average of the corresponding microscopic quantity, but it is related to the inverse of the microscopic dielectric matrix in the following way:

$$\varepsilon_M(\omega) = \lim_{q \rightarrow 0} \frac{1}{\varepsilon_{G=0, G'=0}^{-1}(\mathbf{q}, \omega)}. \quad (4)$$

This formula relies on the fact that although, in an inhomogeneous material, the macroscopic field varies with frequency ω and has a Fourier component of vanishing wavevector, the microscopic field varies with the same frequency but with different wavevectors $q + G$. These microscopic fluctuations induced by the external perturbation are at the origin of the local-field effects and reflect the spatial variation of the material. The microscopic dielectric function is determined, within the linear response theory [16], in the independent-particle picture (RPA, Random Phase Approximation) and using eigenvalues and eigenvectors of a one-particle scheme (as DFT or GW) [17]. There is also a different formulation to include local-field effects in the macroscopic dielectric function, that becomes useful when we will introduce, in the following, the electron-hole interaction in the polarization function. This formulation allows us to include, via the Bethe–Salpeter equation, excitonic and local-field effects on the same footing, and avoid inverting the microscopic dielectric matrix. The complete derivation can be found in Appendix B of Ref. [4].

Up to now we have treated the quasi-particles as non interacting. To take into account the electron–hole interaction, we need to include a higher order vertex correction in the polarization or, in other words, solve the Bethe–Salpeter equation (BSE), which describes the electron–hole pair dynamics. As well explained in the Ref. [4], the BSE can be written as a linear problem whose hamiltonian is given by:

$$H_{\text{exc}}^{(n_1, n_2), (n_3, n_4)} = (E_{n_2} - E_{n_1}) \delta_{n_1, n_3} \delta_{n_2, n_4} - i(f_{n_2} - f_{n_1}) \\ \times \int d\mathbf{r}_1 d\mathbf{r}'_1 d\mathbf{r}_2 d\mathbf{r}'_2 \phi_{n_1}(\mathbf{r}_1) \phi_{n_2}^*(\mathbf{r}'_1) \Xi(\mathbf{r}_1, \mathbf{r}'_1, \mathbf{r}_2, \mathbf{r}'_2) \phi_{n_3}^*(\mathbf{r}_2) \phi_{n_4}(\mathbf{r}'_2).$$

The kernel Ξ contains two contributions: \bar{v} , which is the bare coulomb interaction where the long range part corresponding to vanishing wave vector is not included, and W , the attractive screened coulomb electron–hole interaction. Using this formalism and considering only the resonant part of the excitonic hamiltonian [4], the following expression for the macroscopic dielectric function can be obtained [4]:

$$\varepsilon_M(\omega) = 1 + \lim_{q \rightarrow 0} v(\mathbf{q}) \sum_{\lambda} \frac{\left| \sum_{v, c; \mathbf{k}} \langle v, \mathbf{k} - \mathbf{q} | e^{-i\mathbf{q}\mathbf{r}} | c, \mathbf{k} \rangle A_{\lambda}^{(v, c; \mathbf{k})} \right|^2}{(E_{\lambda} - \omega)}. \quad (5)$$

In Eq. (5) the dielectric function, differently from the RPA approximation, is given by a mixing of single particle transitions weighted by the excitonic eigenstates A_{λ} . Moreover the excitation energies in the denominator are changed from $\varepsilon_c - \varepsilon_v$ to E_{λ} eigenvalues of the excitonic Hamiltonian.

The excitonic calculation is in general, from the computational point of view, very demanding because the matrix to be diagonalized can be very large. The relevant parameters which determine its size are the number of \mathbf{k} points in the Brillouin Zone BZ, the number of the valence bands N_v and the number of conduction bands N_c which build the basis set of pairs of states.

All calculations performed in insulators and semiconductors, show that the inclusion of the electron–hole coulomb interaction allows a more quantitative comparison with experiment, not only below the electronic gaps, where bound excitons are generally formed, but also above the continuum edge. Here we present the optical response of bulk Germanium within GW approximation and including excitonic ef-

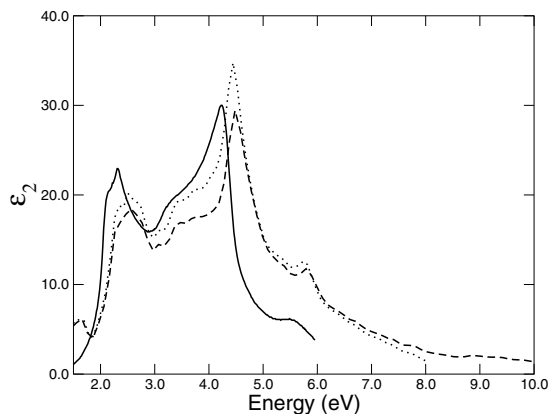


Fig. 1 Imaginary part of the dielectric function of bulk Ge: experimental curve from Ref. [18] (solid line), the GW-RPA curve (dashed line), and also with the inclusion of excitonic (EXC) and local-field effects (LFE, dotted line).

fects. In Fig. 1 we compare the imaginary part of the bulk dielectric function with the experimental curve [18]. Although this example is not as explicit as bulk Si [19] (where the strong effect is essentially due to parallel bands along ΓX direction), this figure shows how the agreement improves with the inclusion, beyond the self-energy corrections, of both local-field and excitonic effects. The e–h interaction may also induce a redshift of the spectral peaks, which partially cancels the blue-shift arising from the self-energy corrections. Our BSE spectrum essentially agree with that obtained by S. Botti et al. in Ref. [20], while a slight blue-shift of the E_2 peak is present with respect to the result reported in Ref. [21], where a static dielectric constant has been used to screen the electron–hole interaction.

3 Low dimensional systems

To illustrate first principles optical properties calculations, we present the results for two low dimensional systems: the heterocyclic organic molecule pyrrole, C_4H_5N , and the Ge nanowires (Ge NWs). In both cases the inclusion of local-field effects induces large changes in the calculated spectra.

Pyrrole is comprised of a five-atom aromatic ring with six π electrons: two are donated by nitrogen, and one from each of the four carbon atoms. This molecule is a fundamental unit in many important biological systems, such as porphyrins and phthalocyanines. In our calculation we first optimized the geometrical structure of the molecule (Fig. 2), within a supercell of size $35 \times 35 \times 35$ a.u., obtaining values in good agreement with Ref. [22]. We can qualitatively compare our calculated optical spectra with the experimental VUV absorption spectrum (Fig. 3(a)), which is characterized by two main broad peaks, the first at about 6 eV, the second at 7.5 eV [23]. In Fig. 3(b) we report the calculated (averaged over orientation) DFT-LDA, GW, and DFT-LDA + LFE optical absorption spectra of the isolated molecule. The DFT spectrum shows three peaks, that do not agree with the experimental result, both in the energy position (the absorption threshold is at 5 eV, due to the DFT underestimation of HOMO–LUMO gap), and in the overall lineshape (with a wrong relative intensity for the structures). Preliminary GW calculations give an opening of the gap of about 3 eV. The optical spectrum is shifted towards higher

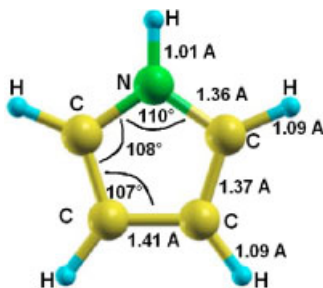


Fig. 2 (online colour at: www.pss-b.com) Geometrical structure of pyrrole, obtained with DFT-LDA calculation.

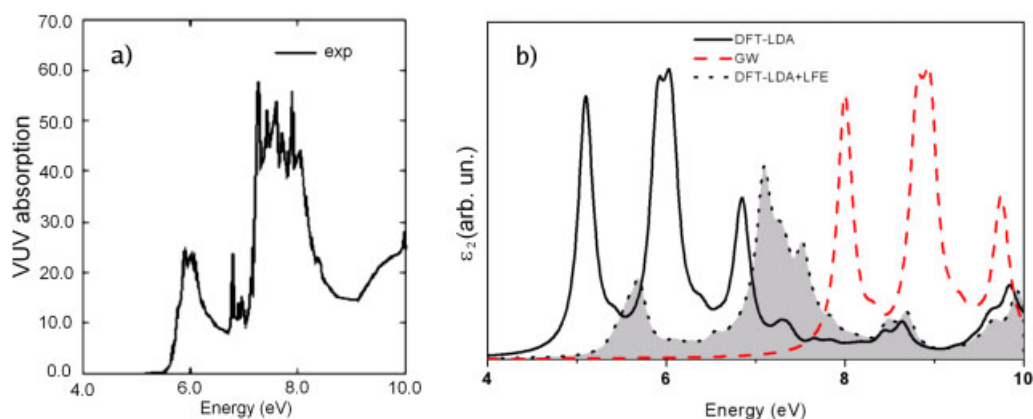


Fig. 3 (online colour at: www.pss-b.com) a) Experimental absorption spectrum of pyrrole from Ref. [23]. b) DFT-LDA (solid line), GW (dashed line), and DFT-LDA + LFE (grey, dotted line) optical spectra for pyrrole molecule.

energies, with the first absorption peak at about 8 eV, but the relative weight of the structures is unaffected. The quasi-particle calculation clearly overcorrects the underestimation of the DFT level, without improving the shape of the spectrum.

On the other hand, the local-field effects correct the shape with respect to the DFT result, through a redistribution of the intensity. In the DFT-LDA + LFE spectrum, we have two structures, the first centered at 5.7 eV, the second at 7.3 eV, at energies comparable to the experimental ones. In addition their relative weights reproduce well the experimental result, with the second peak twice as intense as the first. The inclusion of electron–hole screened interaction, which almost cancels the blue-shift due to the self-energy corrections, will be discussed separately [24]. Here we aim to underline that the good agreement with the experimental spectrum obtained at DFT-LDA + LFE level is not surprising. In fact the compensation of self-energy corrections and electron–hole interaction has been predicted theoretically by Delerue et al. [25] and observed by Porter and co-workers [26] in zero-dimensional nanomaterials. Moreover it is very well known that the Time Dependent Density Functional Theory [27], within the LDA approximation (TDLDA), is generally very accurate to describe excited states for small zero-dimensional systems like molecules and nanoclusters. It has been already discussed [4] that the inclusion of local-field effects, for such systems, is essentially equivalent to perform TDLDA calculations. The (neglected) local LDA exchange–correlation kernel, which describes many-body effects, is indeed small with respect to the unscreened coulomb potential, which describes local-field effects.

As a final example we discuss some of the results obtained for isolated hydrogen-terminated germanium wires oriented along the [100], [111] and [110] directions, with an effective width of 4 Å, 8 Å and 12 Å. An extended discussion about these wires, including electron–hole interaction effects, is presented elsewhere [28]. A graphical representation of the small section wires is reported in panel (a) of Fig. 4.

Starting with a study of the atomic relaxation effect on the wire band structures and dielectric response, which we found to be very small, we obtained DFT-LDA bandstructures. Our results are consistent with previous theoretical calculations [29] obtained within a LAPW approach instead of a Pseudo-Potential one (used to obtain all the results presented here). No hydrogen-induced states appear within the band gap region for all the Ge NWs oriented along the three directions. The hydrogen saturation of the dangling bonds provides a smooth termination of the orbitals, similar to a boundary condition at the interface with a wide gap material, but does not play a role in the electronic properties of the Ge NWs, since the hydrogen-related states appear at energies far from the energy range of the gap. We observe an anisotropy in the fundamental band gap with respect to the wire orientation and moreover we find that the bandstructures are weakly affected by the atomic relaxation. As in Ref. [29] we find a clear direct gap at Γ in the [110]-oriented wires, induced by quantum confinement effects, that makes this type of wire

Table 1 Direct DFT-LDA band gaps at Γ . When the minimum gap is indirect we report its value on the third and fourth column.

wire orient.	wire size	direct ideal	direct relaxed	indirect ideal	indirect relaxed
[100]	0.4 nm	3.93	3.95	3.87	3.92
	0.8 nm	2.60	2.54		
	1.2 nm	1.85	1.85		
[110]	0.4 nm	2.21	2.13		
	0.8 nm	1.27	1.33		
	1.2 nm	0.90	0.87		
[111]	0.4 nm	3.43	3.49	3.24	3.26
	0.8 nm	2.12	2.14	2.09	2.09
	1.2 nm	1.55	1.57	1.53	1.53

suitable for photoluminescence applications; whereas for the other two orientations we find a small difference between direct and indirect minimum gaps, but in all cases the wires remain characterized by an indirect fundamental gap. This is at variance with the case of Si NWs, where direct band gaps at Γ were found for [100], [110] and [111] oriented wires [30–32]. This difference is due to quantum confinement effects on the conduction band minima, that in the two bulk semiconductors are differently located. In Si they occur in the [100] directions about 80% of the way to the zone boundary, in Ge along the [111] directions centered on the midpoints of the hexagonal zone faces. In Table 1 we show in detail all the values of the electronic DFT-LDA gaps for the ideal (unrelaxed) and relaxed structures; when the minimum gap is indirect we explicitly report its value in the third (unrelaxed) and fourth (relaxed) column. In order to emphasize the dependence of band gaps not only on the size of the wires but also on the different orientations we plot the values of the electronic DFT-LDA direct gaps in panel (b) of Fig. 4.

In Fig. 5 we plot some optical spectra for the [110] oriented wires ($d = 4 \text{ \AA}$, 8 \AA), calculated at the independent-particle level with and without the inclusion of local-field effects. This shows how the dielectric response is strongly modified, in these confined 1D systems, by taking into account their inhomogeneity (RPA + LFE). In particular, including the local-field effects, we observe a small change in the optical spectrum for light polarized along the wire axis (x -direction, left panels), while we find an important intensity reduction for the perpendicular light polarization (y -direction, right panels). Similar behaviour has been observed in other 1D systems, like nanotubes, by other groups using the same ab-initio

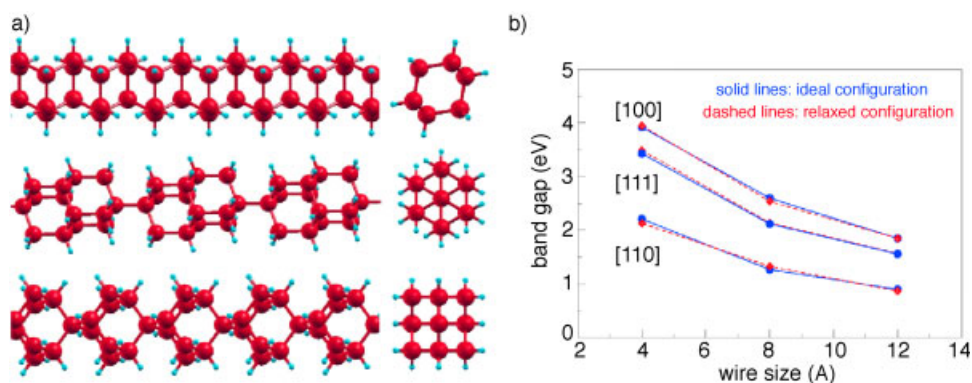


Fig. 4 (online colour at: www.pss-b.com) a) Geometrical structures of the 0.4 nm Ge wires in the [110] (top), [111], and [100] (bottom) directions shown from the side (left) and from the top (right). Large spheres represent Ge atoms; small spheres are hydrogen atoms used to saturate the dangling bonds. b) Plot of the DFT-LDA direct band-gaps as a function of the wires size, with (diamonds) and without (circles) atomic structural relaxation.

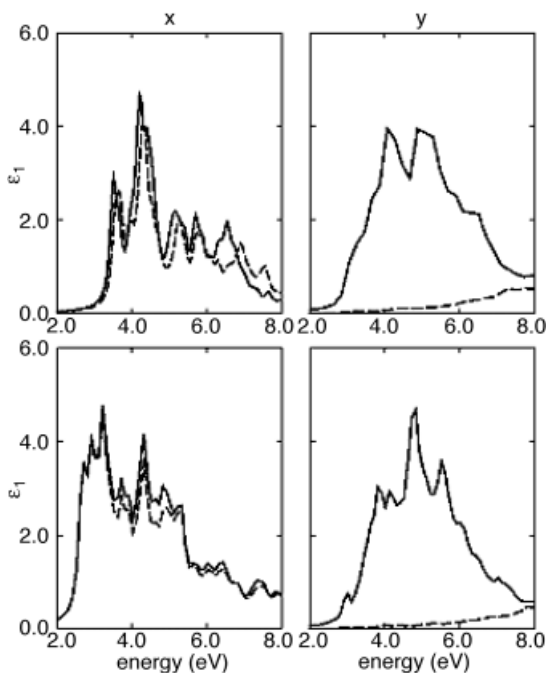


Fig. 5 Theoretical imaginary part of the dielectric function for light polarized in the direction of the wire axis (left panels), and perpendicular to it (right panels), for [110] oriented wires with different sizes: 4 Å (upper panels), 8 Å (lower panels). Solid lines: RPA; dashed lines: RPA + LFE.

approaches [33, 34]. The reason why the RPA, without LFE, fails in the direction perpendicular to the wire axis is due to the depolarization effect which is created by the polarization charges induced in the system [33]. The depolarization is accounted for only if LFE are included, and is responsible for the suppression of the low energy absorption peaks in the y direction, rendering the wire almost transparent in the studied energy window. Moreover an interesting point, shown recently by F. Bruneval et al. [35], is that the local-field effects obtained with the ab-initio techniques described in the present manuscript, can be reasonably taken into account by means of a classical effective-medium theory (EMT): in fact they have shown, for Si nanowires, that the dielectric function, corresponding to the perpendicular and the parallel directions, experiences similar changes to those obtained with ab-initio calculations, when the Maxwell–Garnett equation, for one-dimensional systems, is applied to the dielectric function of Si bulk [35].

In Ref. [28] other spectra, obtained overcoming the random phase approximation, but including both self-energy corrections and e – h interaction, show very important band-gap opening, two or three times bigger than in bulk Ge, as well as very strong e – h interactions. Furthermore a significant cancellation of self-energy and electron–hole interaction effects (as seen from the onset of the optical spectrum) has been observed in the [111] and [100] oriented wires which have a quasi zero-dimensional character, appearing as a collection of small clusters connected along the axis [28].

4 Conclusions

The first-principles theoretical and computational scheme, obtained from a combination of density functional and many body perturbation theories, which nowadays allow the calculation of both ground and excited state properties of many materials, has been summarized here. Some examples of low dimensional system optical spectra, where many-body effects strongly influence the dielectric response, have also been given.

Acknowledgements This work was funded in part by the EU’s 6th Framework Programme through the NANO-QUANTA Network of Excellences Grant No. NMP4-CT-2004-500198d. We acknowledge CINECA CPU time granted by INFN.

References

- [1] P. Hohenberg and W. Kohn, Phys. Rev. **136**, B864 (1964).
[2] L. Hedin, Phys. Rev. **139**, A796 (1965).
[3] R. M. Dreizler and E. K. U. Gross, Density Functional Theory (Springer Verlag, Heidelberg, 1990).
[4] G. Onida, L. Reining, and A. Rubio, Rev. Mod. Phys. **74**, 601 (2002).
[5] M. Rohlfing and S. G. Louie, Phys. Rev. B **62**, 4927 (2000).
[6] W. Kohn and L. J. Sham, Phys. Rev. **140**, A1133 (1965).
[7] D. M. Ceperley and B. J. Alder, Phys. Rev. Lett. **45**, 566 (1980).
J. P. Perdew and A. Zunger, Phys. Rev. B **23**, 5048 (1981).
[8] J. P. Perdew, K. Burke, and M. Ernzerhof, Phys. Rev. Lett. **77**, 3865 (1996).
[9] L. Fetter and J. D. Walecka Quantum theory of Many Body Systems (McGraw-Hill, New York, 1981).
R. D. Mattuck, A guide to Feynman diagrams in the many body problem (McGraw-Hill, New York, 1976).
[10] L. Hedin, B. J. Lundquist, in: Solid State Physics, edited by H. Ehrenreich, F. Seitz, and D. Turnbull, Vol. 23 (Academic press, New York, 1969), p. 1.
[11] G. Strinati, Riv. Nuovo Cimento **11**, 1 (1988).
[12] P. M. Echenique, J. M. Pitarke, E. V. Chulkov, and A. Rubio, Chem. Phys. **251**, 1 (2000).
[13] M. S. Hybertsen and S. G. Louie, Phys. Rev. B **34**, 5390 (1986).
[14] R. W. Godby, M. Schlüter, and L. J. Sham, Phys. Rev. B **37**, 10159 (1988).
[15] S. L. Adler, Phys. Rev. **126**, 413 (1962).
N. Wisser, Phys. Rev. **129**, 62 (1963).
[16] J. Lindhard and K. Dan, Vidensk. Selsk. Mat.-Fys. Medd. **28**, No. 8 (1954).
[17] P is defined as $\delta\rho(x) = \int dx' P(x, x', \omega) \delta V_{\text{tot}}(x')$ where it relates the change in the density due to the perturbation to the total potential (external + induced potential).
[18] D. Aspnes and A. A. Studna, Phys. Rev. B **27**, 985 (1983).
[19] S. Albrecht, L. Reining, R. Del Sole, and G. Onida, Phys. Rev. Lett. **80**, 4510 (1998).
[20] S. Botti et al., Phys. Rev. B **69**, 155112 (2004).
[21] L. X. Benedict, E. L. Shirley, and R. B. Bohn, Phys. Rev. B **57**, R9385 (1998).
[22] R. Burcl, R. D. Amos, and N. C. Handy, Chem. Phys. Lett. **355**, 8 (2002).
[23] B. O. Roos et al., J. Chem. Phys. **116**, 7526 (2002).
M. H. Palmer, I. C. Walker, and M. F. Guest, Chem. Phys. **238**, 179 (1998).
J. Wan, J. Meller, M. Hada, M. Ehara, and H. Nakatsuji, J. Chem. Phys. **113**, 7853 (2000).
[24] L. Chiodo et al., in preparation.
[25] C. Delerue, M. Lannoo, and G. Allan, Phys. Rev. Lett. **84**, 2457 (2000).
[26] A. R. Porter, M. D. Towler, and R. J. Needs, Phys. Rev. B **64**, 035320 (2001).
[27] E. Runge and E. K. U. Gross, Phys. Rev. Lett. **52**, 99 (1984).
[28] M. Bruno et al., Phys. Rev. B **72**, 153310 (2005).
[29] A. N. Kholod et al. Phys. Rev. B **70**, 035317 (2004).
[30] X. Zhao, C. M. Wei, L. Yang, and M. Y. Chou, Phys. Rev. Lett. **92**, 236805 (2004), and references therein.
[31] F. Buda, J. Kohanoff, and M. Parrinello, Phys. Rev. Lett. **69**, 1272 (1992).
[32] A. M. Saitta, F. Buda, G. Fiumara, P. V. Giaquinta, Phys. Rev. B **53**, 1446 (1996).
[33] A. G. Marinopoulos, L. Reining, A. Rubio, and N. Vast, Phys. Rev. Lett. **91**, 046402 (2003).
[34] C. D. Spataru, S. Ismail-Beigi, L. X. Benedict, and S. G. Louie, Phys. Rev. Lett. **92**, 077402 (2004).
[35] F. Bruneval, S. Botti, and L. Reining, Phys. Rev. Lett. **94**, 219701 (2005).